ISBN: 978-3-95450-262-2 ISSN: 2673-5350 doi: 10.18429/JACoW-IBIC2025-WEPMO24

OPTIMIZATION OF PHOTOEMISSION BLADE X-RAY BEAM POSITION MONITOR FOR WIDE RANGE OF UNDULATOR GAP OPERATION*

P. Ilinski†, MAX IV Laboratory, Lund, Sweden

Abstract

Optimization of the photoemission blade type XBPM mostly performed to increase its resolution by increasing the readout signal current and by optimizing blades geometry. This requires tailoring of the XBPM for a particular undulator, making almost every XBPM unique at the Synchrotron Radiation facility. In many cases the calibration coefficient is gap dependent. To overcome those drawbacks an alternative optimization strategy is considered which will help to minimize gap dependence and could provide a unified XBPM design for all XBPM at Synchrotron Radiation (SR) facility.

MAX IV XBPM STATUS

The choice of the undulator parameters dictated by desired beamline operation energy range and current permanent magnets technology. In most cases undulator operates with on-axis magnetic field in the range of 0.7 T to 1.2 T. The required energy range is achieved by a choice of the undulator period, which will define the range (see Fig. 1) of undulator deflection parameter $K = 0.934\ \lambda_u[\mathrm{cm}]\ B[\mathrm{T}]$, where λ_u is undulator period and B is on-axis magnetic field.

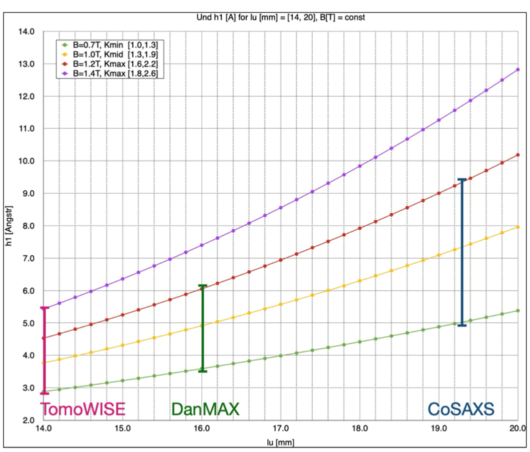

Figure 1: Operation range of the undulator deflection parameter K for the range of on-axis magnetic field B of 0.7-1.2 T.

MAX IV upstream XBPM is located downstream from the frontend first Fixed Mask, which has an exit aperture of 1.0 mrad x 1.0 mrad, second XBPM is located 2.5 m downstream. The XBPMs have a X/Y stage for positioning. Blades geometry is chosen to increase signal and resolution and not to shield second XBPM, Fig. 2.

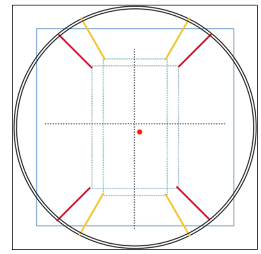

Figure 2: MAX IV NanoMAX XBPMs upstream (red), downstream (yellow) blades orientation relative to the Fixed Mask and XBPM pre-mask.

In most cases, XBPM blades geometry is chosen to maximise spatial resolution [1], which can be achieved by increasing the signal and changing the calibration coefficient. This choice of optimization leads to multiple XBPM configurations with different opening of the blades. Opening of the blades for MAX IV XBPMs is presented at Fig. 3.

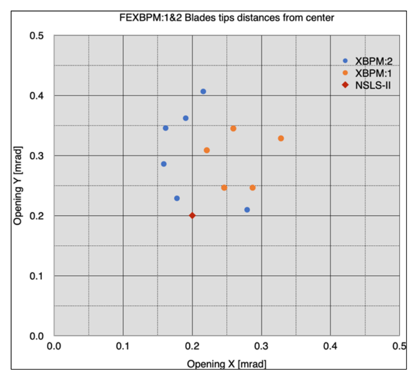

Figure 3: MAX IV XBPM blades opening angle.

MAX IV XBPMs are operated with negative Bias voltage of -120 V applied to the blades. Typical blade current is in the range of 100-300 μA, at which XBPMs are achieving sub-micron spatial resolution. The XBPMs calibration coefficients [mm/au] depend on the undulator gap, this requires XBPM spatial calibration in the gap operation range.

XBPM calibration can be performed by moving the XBPM with X/Y stage or by deviating undulator beam, these approaches may give different results of calibration coefficients. The effect is purely geometrical (Fig. 4), it depends on the blade geometry relative to the upstream aperture. In case of MAX IV NanoMAX XBPM (Fig. 2), calibration in vertical direction using y-stage will be changing exposed by the beam length of the blades, which will lead to a different result compared to the calibration performed with the beam deviation. Since in regular operation the beam is moving relative to the XBPM, it is appropriate to use beam deviation method for XBPM spatial calibration.

* Research conducted at MAX IV is supported by the Swedish Research council (contract 2018-07152), the Swedish Governmental Agency for Innovation Systems (contract 2018-04969), and Formas (2019-02496).
†petr.ilinski@maxiv.lu.se

ISBN: 978-3-95450-262-2 ISSN: 2673-5350 doi: 10.18429/JACoW-IBIC2025-WEPMO24

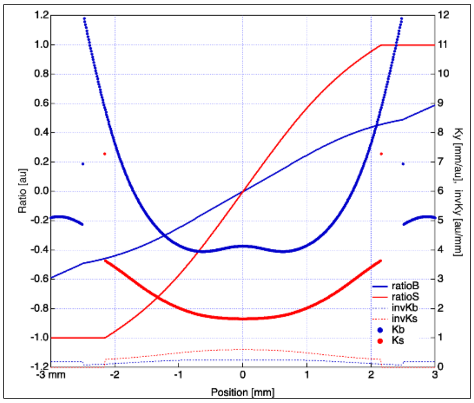

Figure 4: Example of calibration using stage (K_s – red dots) or beam deviation (K_b – blue dots).

OPTIMIZATION OF THE BLADES GEOMETRY

XBPM 2D Signal density can be calculated by multiplying undulator spectra by total electron yield for blade material, which was tungsten. An example of the XBPM 2D Signal density distribution at 10 m for 18 mm period undulator with B = 1.0 T is shown in Fig. 5.

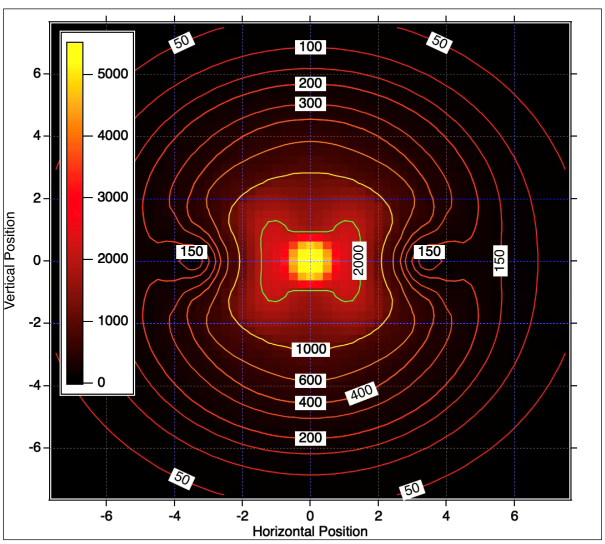

Figure 5: Signal density [μA/mm²] for Tungsten blade at 10 m, 18 mm period undulator, B = 1.0 T.

Calibration coefficients Kx_0 and Ky_0 depend on undulator gap, this requires extensive calibration, which may not be always practical, in particular for EPUs. Since calibration is performed with the beam deviation, the XBPM X/Y stages are not a necessity. A larger spatial operation range can be considered over the resolution optimization. Therefore, an alternative approach is suggested as a goal for photoemission blade XBPM optimization:

- Minimizing calibration coefficient dependency on undulator gap.
- Increased spatial range of operation.
- Same blades geometry for all XBPMs at SR facility.

The calibration coefficients were first calculated from calibration curves, $Kx(x)$ is shown in Fig. 6, $Kx_0 = Kx(0)$.

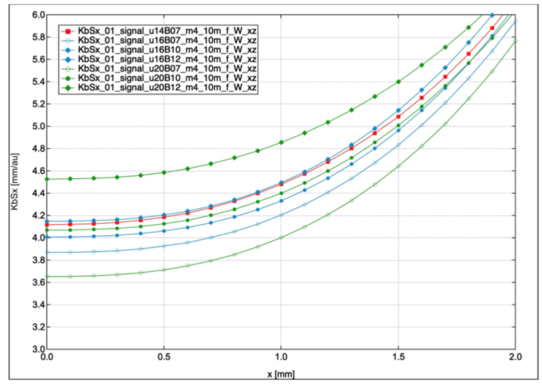

Figure 6: Kx vs x 16 and 20 mm period undulator, and B of 0.7 T, 1.0 T, 1.2 T.

To examine gap dependence, $Kx_0(B_y)$, $Ky_0(B_y)$ were calculated for 16, 18, and 20 mm period undulators at different gaps, with on-axis magnetic field B_y of 0.7 T, 1.0 T, 1.2 T (Figs. 7 and 8).

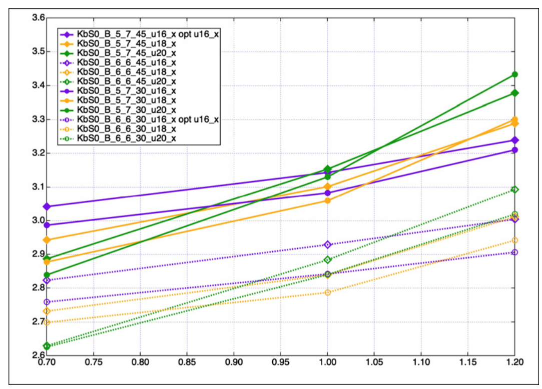

Figure 7: Kx_0 vs B[T] for 16, 18, and 20 mm period undulator, blades opening of 5 mm x 7 mm and 6 mm x 6 mm at 30 and 45 degrees.

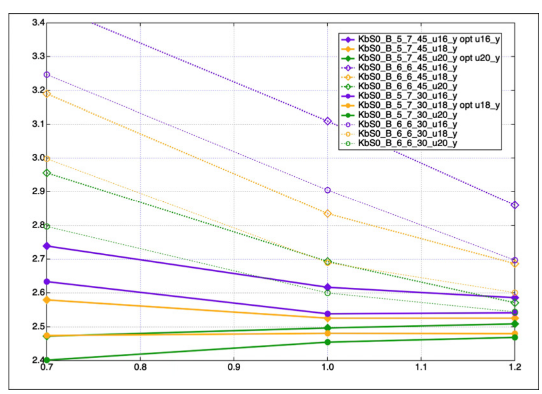

Figure 8: Ky_0 vs B[T] for 16, 18, and 20 mm period undulator, blades opening of 5 mm x 7 mm and 6 mm x 6 mm at 30 and 45 degrees.

To quantify gap dependence, a standard deviation can be calculated for $Kx_0(B_y)$, $Ky_0(B_y)$. Then a 2D distributions of standard deviations $Kx_0(B_y)$, $Ky_0(B_y)$ for blade openings were calculated for 16, 18, and 20 mm period undulators. 2D distributions of standard deviations of $Kx_0(B_y)$, $Ky_0(B_y)$ for 18 mm period undulators is presented for vertical (Fig. 9) and for horizontal (Fig. 10) directions.

ISBN: 978-3-95450-262-2 ISSN: 2673-5350 doi: 10.18429/JACoW-IBIC2025-WEPMO24

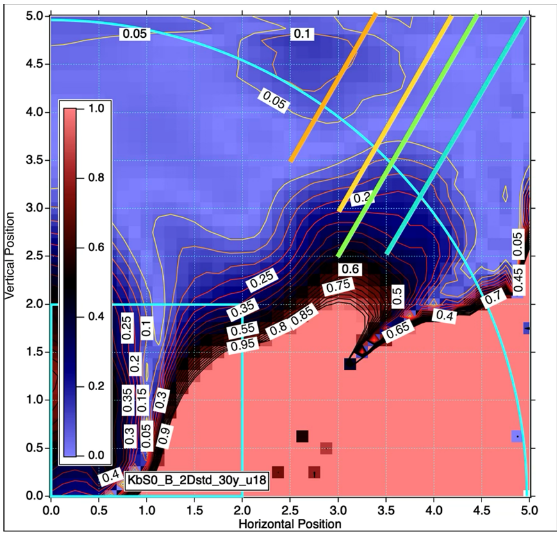

Figure 9: 2D $Ky_0(B_y)$_std, 18 mm period undulator, blade at 30 degrees.

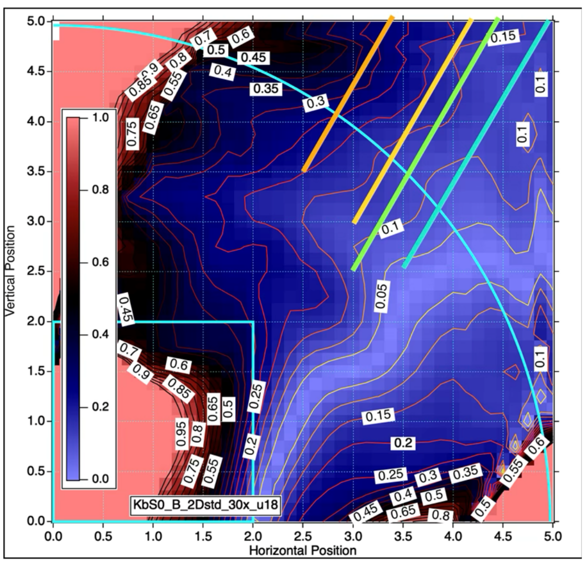

Figure 10: 2D $Kx_0(B_y)$_std, 18 mm period undulator, blade at 30 degrees.

It will be advantageous to place blades so, that $Kx_0(B_y)$, $Ky_0(B_y)$ differences for all undulator gaps will be minimal, which implies minimization of standard deviation. As can be seen from Fig. 9, by choosing a location with small standard deviation for $Ky_0(B_y)$, the blade opening of 5 mm x 7mm (*h* x *v*) is optimal, while for $Kx_0(B_y)$ a 7 mm x 5 mm is preferable. A compromise for both directions can be considered for a 6 mm x 6 mm blade opening. Direct comparison of $Kx_0(B_y)$ and $Ky_0(B_y)$ (Figs. 7 and 8) shows, that blade geometry of 5 mm x 7 mm is a preferred choice for both directions.

Blades will have larger openings for this optimization, which leads to a lower Signal. Also, a choice of the fixed mask exit aperture affects the blade length and therefore the Signal. With square exit aperture the blade length can be too long to satisfy the rigidity. So, a circular exit aperture can be considered, Fig. 11. As can be seen at Fig. 12, Signal current for blades with 6 mm x 6 mm opening will be above 20 μA level for a circular aperture and above 50 μA level for a square aperture which is sufficient to obtain sub-micron spatial resolution.

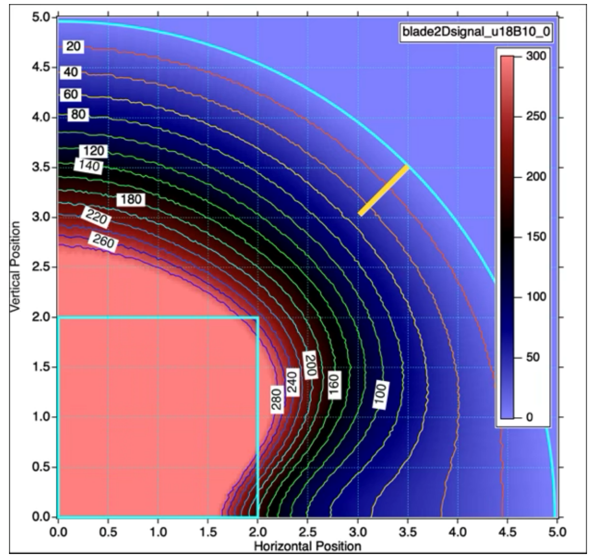

Figure 11: 2D distribution of the Blade Total Signal [μA], 1 mrad diameter aperture, 18 mm period undulator, B = 1.0 T.

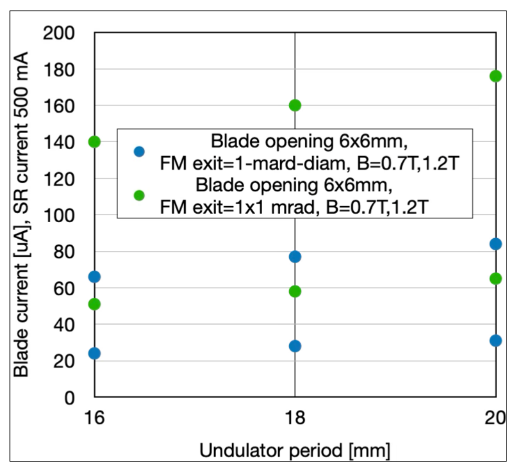

Figure 12: Blade Signal current [μA], opening 6 mm x 6 mm, B = 0.7 T, 1.2 T, fixed mask exit aperture of 1 mrad x 1 mrad (green) and 1 mrad-diameter (blue).

CONCLUSION

As was shown, the XBPM calibration should be preferably performed by the beam deviation, XBPM X/Y stages are not a necessity in this situation. Optimization of the XBPM blades geometry can be performed to minimize undulator gap dependence and to increase operation range with Signal level still satisfying sub-micron spatial resolution.

REFERENCES

[1] P. Ilinski, “Optimization of NSLS-II Blade X-ray Beam Position Monitors: From Photoemission Type to Diamond Detector”, in *Proc. IBIC'13*, Oxford, UK, Sep. 2013, paper MOPC10, pp. 67-70.